Journal of Polymers and the Environment (2023) 31:4801–4816
https://doi.org/10.1007/s10924-023-02835-9

ORIGINAL PAPER

Green Bionanocomposites Based on Polyhydroxybutyrate and Filled with Cellulose Nanocrystals: Melting Processing and Characterization

Anja Schmidt[1,2] · Birgit Bittmann-Hennes[2] · Belén Montero[1] · Bernd Wetzel[2] · Luis Barral[1]

Accepted: 16 March 2023 / Published online: 27 May 2023

Abstract

This article contributes to the understanding of biobased and biodegradable polyhydroxybutyrate (PHB) bionanocomposites melt processed by pre-industrial methods such as extrusion and injection molding and reinforced by weight contents of 1 and 3 wt% of cellulose nanocrystals (CNC) derived from waste streams of the paper industry. Ultrasonic treatment was used for dispersion of the CNC, which was followed by transmission electron microscopy. The thermal properties and the crystallization behavior of bionanocomposites were studied by thermogravimetric analysis, differential scanning analysis, X-ray diffraction and polarized optical microscopy. Investigations on the bending properties were carried out in conjunction with the analysis of their dynamic mechanical behavior. Scanning electron microscopy was used to characterize the fracture surface. All these analyses give a deep insight into their structure-property relationship. The moisture absorption measurements and gas barrier properties analysis made to the processed bionanocomposites have provided an insight into their behavior under environmental conditions. The PHB bionanocomposites with a low content of 1 wt% CNC were found to have the best dispersion quality, which had a positive effect on almost all mechanical and thermal properties. The increase in crystallinity with the incorporation of CNC also contributed to an improvement in mechanical properties. In addition, the bionanocomposites show a slightly lower tendency to absorb moisture and better barrier properties to oxygen and water vapor. These findings showed that these bionanocomposites are suitable for use in the packaging industry.

✉ Belén Montero
belen.montero@udc.es

[1] Present Address: Universidade da Coruña, Group of Polymers, Physics and Earth Sciences Department, Campus Industrial de Ferrol (CIF), CITENI, Escuela Politécnica de Ingeniería (EPEF), Campus de Esteiro. C/ Mendizabal s/n, 15403 Ferrol, A Coruña, Spain

[2] Leibniz-Institut für Verbundwerkstoffe GmbH, Erwin-Schrödinger-Str. Geb. 58, 67663 Kaiserslautern, Germany

Graphical Abstract

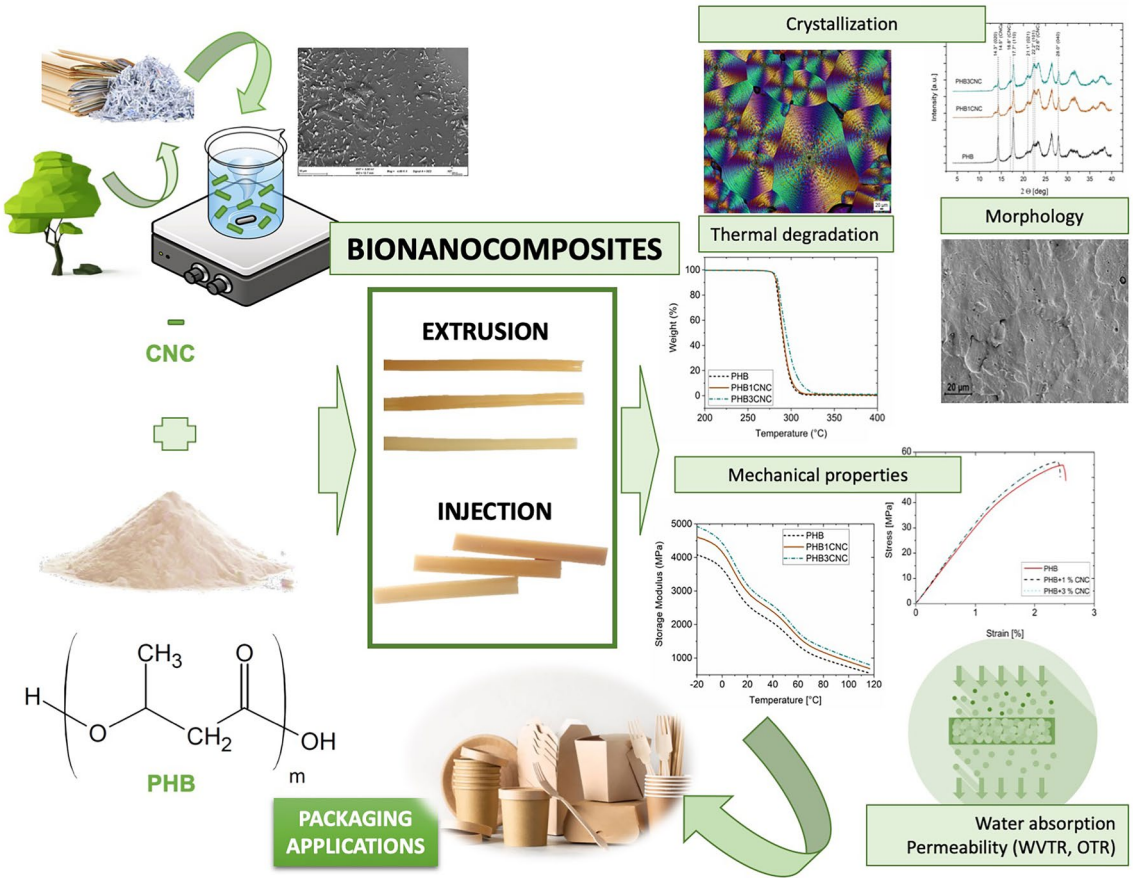

Keywords Bionanocomposites · Cellulose nanocrystals · Poly(3-hydroxybutyrate) · Mechanical properties · Thermal behavior · Barrier properties

Introduction

Biobased polymers and their composites are one of the answers to the depletion of mineral oil. As a consequence of their increased demand for these alternatives, this market has been growing strongly in recent years [1]. The constantly widening areas of application range extends from the automotive and construction sectors to electronic devices, sports and leisure, as well as packaging materials [2, 3]. Biocomposites, which are at the same time biodegradable, can in addition contribute to the reduction of greenhouse gas emissions [4]. Complementary to these features, the increasing customer demand for environmentally friendly products is further supporting the growth of the biopolymer market segment.

However, many biopolymers still suffer from drawbacks, such as high prices and moderate mechanical and thermal properties, which limit their range of applications. Blending of two or more polymers can be a solution to adjust the bioplastics' property profile [5]. Another approach is the reinforcement of biopolymers by particles or fibers [6, 7]. The combination of blending and particle reinforcement for dispersion and property adjustment was also investigated [8].

Polyhydroxybutyrate (PHB) belongs to the group of polyhydroxyalkanoates (PHAs), which comprises a family of linear biopolyesters. PHAs can be extracted from the cytoplasm of various bacteria and are biodegradable under both aerobic and anaerobic conditions [9]. PHB is the simplest structure belonging to the PHA family. It is non-toxic and biocompatible, but its obtaining has high costs. Great efforts are being made to reduce these costs and getting a competitive PHA production [10]. So, in recent years Hempel et al. [11] showed that PHAs, i.e. PHB, can also be extracted from microalgae with a great potential of higher yield.

The properties showed by PHB such as crystallinity degree, melting and glass transition temperatures, strength and modulus, are comparable to those of polypropylene, and the material can be processed by conventional melt

processing techniques, such as extrusion, injection molding, thermomolding, 3D printing [12]. Moreover, PHB shows a good resistance to moisture and a higher oxygen barrier performance than polyolefins. All these characteristics make PHB an attractive material as substitute for synthetic polymers. However, PHB in its native form exhibits some shortcomings such as brittleness and limited processability window [13].

Nanocellulose is a structural polysaccharide, which can be extracted from various sources such as e.g., wood pulps, sawdust waste, cotton, corn, flax or jute fibers as well as used paper. Although this environmental benign material has plenty of potential applications, among them in the energy and in the food sector, few developments have yet found their way into commercial use [14, 15]. Cellulose nanocrystals with a rod-like morphology and a high aspect ratio are obtained by acid hydrolysis of amorphous regions of cellulose fibers. Dimensions and aspect ratio depend on the vegetal source used to get the cellulose and the acid hydrolysis conditions [16]. Cellulose nanocrystals have been studied as nanofiller in different polymeric matrices to improve the thermal and mechanical properties as well as to improve moisture resistance and to reduce swelling [6]. Yu et al. [17] found a direct relation between the enhancement in mechanical properties of bionanocomposites and both, the aspect ratio of cellulose nanocrystals and their distribution within the matrix. The improvement of mechanical properties due to the nanoscale dimensioning of fillers and the high reactivity of cellulose molecules has already been described in other publications for use in composites [18]. Terms as the nanoscale dimension of the filler and the high reactivity of cellulose molecules were considered as factors improving mechanical properties in the bibliography as well. In fact, Panaitescu et al. [19] obtained higher Young's modules as well as improved thermal properties by the addition of wood waste fibers (CF) to PHB matrices. Arrieta et al. [20] found that a better dispersion of cellulose nanocrystals in PLA-PHB blends increased the elongation at break, enhanced the crystallization effect and improved the oxygen barrier. Moreover, the use of cellulose nanoparticles as nucleating agent was demonstrated to improve the crystallinity and to have an influence on thermal and mechanical composite properties [6].

For this study PHB was chosen as matrix material and nanocellulose as reinforcing filler with the objective of obtaining fully biobased and biodegradable composites. Recent studies on biotechnological strategies for the improvement of PHB's production process bear good prospects of leading to manufacturing price reductions for these biopolymers, thus, increasing their potential applications [21]. Moreover, the combination of CNC and PHA's in polymer composites showed promising improvement of mechanical and thermal properties as well as moisture resistance, heat distortion temperatures and biocompatibility [22, 23]. However, to take advantage of these benefits, it is important to ensure good dispersion of the particles. Therefore, during the production of the bionanocomposites, an efficient functionalization of the CNC is required to avoid the formation of agglomerates. To this end, the use of dispersants and compatibilizers, among others, is being tested, but these may have a negative impact on final costs and on biocompatibility as well as biodegradability. However, most studies used solution casting for sample manufacturing, which involves toxic solvents for PHA´s and are limited to laboratory scale [24].

The aim of this study was the manufacturing of PHB based bionanocomposites with two different weight contents of crystalline nanocellulose by scalable melt mixing procedures, such as extrusion and injection molding, without the need for using toxic solvents. The analysis of the morphology and crystallization behavior of these bionanocomposites was made. To complete this study, the investigation of their thermal and mechanical properties together with their behavior under environmental conditions, through the study of their moisture absorption and their water vapor and oxygen barrier properties, was analyzed. A better understanding of the structure-property relationship of these materials can foster their application as alternative for petroleum based and non-degradable materials in packaging as well as technical applications.

Materials and Methods

Materials

Polyhydroxybutyrate (PHB) powder was purchased from the company Biomer (Germany) under the trade name P338. The polymer has a purity of 98% and a melting temperature of 180 °C according to the supplier. Cellulose nanocrystal (CNC) water suspension with 3 wt% CNC is kindly provided by Melodea Ltd. (Israel). The CNC is derived from the sludge of the pulp and paper industry and is provided in aqueous suspension with a sulfur content of around 114 mmol kg^{-1}. The CNC particles show a rod-like morphology. According to the supplier, the particles' diameter lies between 5 and 20 nm while their length ranges between 100 and 500 nm. The CNC's relative density ranges between 1.0 and 1.1 g cm^{-3}.

Bionanocomposite Manufacturing

First of all, the stability of the CNC water suspension was ensured by ultrasonification and this ultrasonic stabilized CNC water suspension was further diluted with 200 mL of distilled water Thereby, the used ultrasonic treated

nanocellulose suspension should ensure good dispersion at small contents in the matrix avoiding the CNC agglomeration. Prior to processing, corresponding amounts of PHB powder and diluted CNC water suspension to get materials with CNC proportions of 1 and 3 wt% were mixed by a laboratory mechanic stirrer during 20 min. This mixture was dried in the oven at 60 °C for 48 h in order to evaporate the water previously to the processing. The samples were monitored using a moisture balance. The resulting powders were further processed by melt mixing.

Bionanocomposites, with 1 wt% (PHB1CNC) and 3 wt% (PHB3CNC) CNC filler contents, considered low enough for preventing the CNC agglomeration, were prepared by melt mixing by means of a Haake MiniLabII extruder from Thermo Fisher Scientific Inc. (USA). Extrusion were performed at 178 °C for 5 min at a speed of 80 rpm. Subsequently, extruded materials were injection molded by a Cronoplast S.L. Babyplast 6/10PT machine from the company Christmann Kunststofftechnik GmbH (Germany). The samples were injected at a temperature of 180 °C, a mold temperature of 50 °C, a 12 mm piston with 1800 bar and an injection time of 2 s and cooling time of 20 s. Bending test samples according to DIN EN ISO 178 with a height of 4 mm, width of 10 mm and length of 80 mm were processed. To precondition the samples, they were stored for three weeks prior to testing. Reference material, without CNC nanofiller added (PHB), was also manufactured in the same conditions.

In this study melt processing was chosen due to the potential industrial up-scaling of this manufacturing method. Some of the processed samples were compression-molded using a hot press (IQAP LAP PL-15, Spain) at a pressure of 60 bar for 7 min and temperatures of 180 °C to perform the barrier tests.

Characterization

Transmission Electron Microscopy (TEM)

In order to understand the dispersion of crystalline nanocellulose in the PHB matrix, TEM images were taken. The transmission electron microscope is JEOL JEM 2010 (JEOL Inc., USA), which was operated at an accelerating voltage of 100 keV. A staining treatment with uranyl acetate 2% solution was made to obtain the images of CNC water suspension.

Thermogravimetric Analysis (TGA)

The CNC and the bionanocomposite materials were explored by means of thermogravimetric analysis (TGA) on a DTG-60 device from Shimadzu (Japan). Samples of about 30 mg were heated from 30 to 400 °C at a heating rate of 10 °C min^{-1} under inert nitrogen atmosphere. The evolution of sample mass in dependence on the temperature was registered.

Differential Scanning Calorimetry (DSC)

The thermal properties of the bionanocomposite materials were investigated using a DSC 3 from Mettler Toledo (Germany). Samples of around 18 mg under a Nitrogen flow of 30 mL min^{-1} were subjected to two heating scans and an intermediate cooling scan. During the first heating scan starting at − 10 °C and ending at 200 °C with a heating rate of 10 ºC min^{-1}, the thermal history of the samples and any residual stresses are erased. The cooling scan from 200 to − 10 °C with a cooling rate of 30 °C min^{-1} serves to analyze the crystallization behavior of the bionanocomposites. The melting behavior can be observed during the second heating scan in which the sample is heated from − 10 to 200 °C with a heating rate of 10 °C min^{-1}.

The samples' degree of crystallinity χ_c was calculated using Eq. (1) and taking into account the heat of fusion of 100% crystalline PHB $\Delta H_0 = 146$ J g^{-1} [25]:

$$\chi_c = \frac{\Delta H_f}{\Delta H_0 \cdot \varphi} \cdot 100 \quad (1)$$

ΔH_f is the heat of fusion of the sample measured by DSC and φ is the weight fraction of PHB.

X-ray Diffraction (XRD)

The crystalline structure of the bionanocomposites was performed using wide angle X-ray diffraction (XRD) with a Siemens D5000 diffractometer (Germany). The analysis was realized at a current of 30 mA at a voltage of 40 kV. A copper anode K-alpha (Cu K_α) with an average wavelength of λ (K_α) = 1.5418 Å was used in the instrument. The scans were made in 2θ range from 5° to 40°, at scanning step rate of 0.75°/min.

The crystallinity fraction was determined by the ratio of the crystalline area of the diffraction peaks to the complete area of the diffractogram according to the Ruland Vonk method [26] Eq. (2):

$$X_c\,[\%] = \frac{I_c}{I_c + I_a} \times 100 \quad (2)$$

Where I_c is the sum of the areas under the crystalline peaks and I_a is the area under the amorphous halo obtained by the Gaussian approach to all the diffractograms. The XRD data were processed through Fityk® 0.9.3 software.

Scherrer's equation was used to calculate the crystal size. The crystal size of the (0 2 0) lattice plane was calculated using Scherrer's Eq. (3):

$$D_{hkl} = \frac{k\lambda}{\beta \cos(\theta)} \quad (3)$$

Where D_{hkl} is the crystal size in normal direction to the hkl lattice plane, k is Scherrer's constant (here given with k = 0.9), λ is the Cu Kα radiation wavelength (1.5418 Å), and β is the full width at half maximum of the Peak in radians [27]. The analysis was performed using Origin Pro 2018.

Polarized Optical Microscopy (POM)

The crystal growth of all materials was analyzed by a DM 2500 M optical polarized microscope from Leica (Germany). Prior to analysis, the samples were cut into slides of 20 µm thickness by means of a HM 350 S Microtome from Microm (Germany). Samples were heated from room temperature to 210 °C with a heating rate of 30 °C min^{-1} using a THMS 600 temperature-controlled stage from Linkam (UK). After holding the temperature for 2 min at 210 °C in order to melt all remaining polymer crystals, the samples were cooled down to room temperature at a cooling rate of 20 °C min^{-1}. During this cooling step, photos were taken every 5 s to record the materials' crystallization behavior.

Three-Point Bending Test

Three-point bending tests of the biopolymer and the bionanocomposites were performed according to testing standard DIN EN ISO 178 using a Zwick 1474 testing machine from the company Zwick (Germany). The rectangular specimens of the dimensions 4 mm × 10 mm × 80 mm were subjected to a preload of 0.1 MPa. Subsequently, they were tested at a velocity of 2 mm min^{-1}. Five samples of each material were tested and the mean values and standard deviations for their bending parameters were calculated.

Scanning Electron Microscopy (SEM)

Cellulose nanocrystals' as well as bionanocomposites' morphology were investigated by scanning electron microscopy (SEM). In case of bionanocomposites, the samples were fractured after being cooling in liquid nitrogen to get the morphology of the fractured surfaces. To prevent charging of the samples, gold sputtering was applied prior to analysis. A Supra 40VP Gemini SEM from Carl Zeiss Microscopy GmbH (Germany) was used to obtain images at an acceleration voltage of 5 keV.

Dynamic Mechanical Analysis (DMA)

The dynamo mechanical tests were made using a dynamic mechanical analyzer from Perkin Elmer, DMA 7 (Massachusetts, USA). Specimens of 1 mm × 15 mm × 4 mm were tested in the three-point bending mode. The dynamic storage modulus (*E'*) and the loss factor (*Tan δ*) were measured as a function of temperature from − 20 °C to 120 °C at a heating rate of 5 °C min^{-1} and a frequency of 1 Hz under a helium atmosphere. Six replicates of each sample were tested.

Moisture Absorption Test

Moisture absorption of the samples was measured according to DIN EN ISO 62. Prior to the analysis the specimens of the dimensions of 10 mm × 4 mm × 40 mm were dried in an oven at 60 °C for 24 h. Subsequently, the materials were stored in a dark recipient with distilled water. At defined times the specimens were removed from the water, dried with a soft paper, and weighed. The sample's moisture absorption M(t) was determined by means of Eq. (4):

$$M(t) = \frac{m_t - m_o}{m_o} \cdot 100 \quad (4)$$

m_0 being the dry sample's mass at the beginning of the experiment and m_t the mass at time t. Five samples of each material were analyzed by this method.

Barrier Properties

Using a hot press, films of (100 ± 10) µm were produced and tested for the measurement of their barrier properties. The film surface was reduced to a test area of 5 cm^2 that was defined by a metal mask sealed by epoxy glue. The tests were recorded in continuous mode.

The oxygen vapor transmission rate (OTR) measurements were performed according to ASTM DIN-3985 using a Mocon OX-TRAN® model1/50G apparatus (Mocon, USA). The films were measured at 23 °C with 3% relative humidity (RH) under 15 psig (77.6 cm Hg) of pressure.

The water vapor transmission rate (WVTR) was measured with a Permatran-W®, model 1/50 G, Mocon equipment, (Mocon Inc., USA) complying the ASTM E-398 standard. The films were measured at a cell temperature of 37.8 °C. Relative humidity of 10% and 100% were applied in two sides of the films as driving force of the test.

Results and Discussion

Transmission Electron Microscopy (TEM)

To investigate the dispersion of the nanofiller into the PHB matrix, pure CNC, neat PHB and the bionanocomposites were examined by TEM and representative images are shown in Fig. 1. The image of pure CNC (Fig. 1a) shows a cluster of rod-like particles of CNC with lengths about

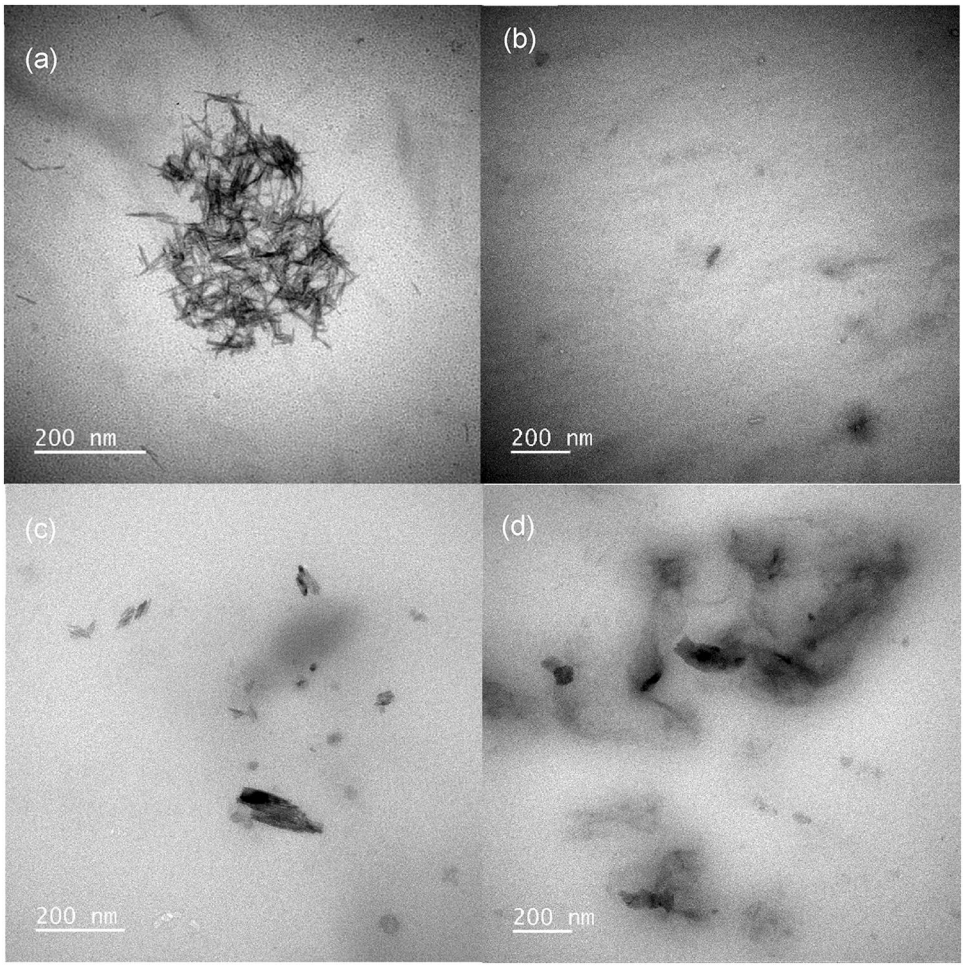

Fig. 1 TEM image of pure CNC (**a**) neat PHB (**b**), PHB with 1 wt% CNC (**c**) and PHB with 3 wt% CNC (**d**)

200 nm, which is in good agree with the data given by the supplier. In neat PHB (Fig. 1b), there are impurities. It is assumed that these impurities are residues from bacteria cell walls as was explained by Bittmann et al. [28]. The addition of 1 wt% CNC (Fig. 1c) reveals the presence of rod-like cellulose particles of different sizes, a bigger one can be seen in the size range defined by the CNC supplier (100–500 nm) and according to the seen in the images obtained from CNC dispersion in Fig. 1a accompanied by other smaller ones, with lengths less than 200 nm, which maintain the rod-like shape. In PHB with 3 wt% CNC (Fig. 1d) CNC agglomerates are appreciated in the upper side of the image. This indicates a better dispersion of the nanocellulose in bionanocomposites with 1 wt% CNC.

The reduction in particle size could have been brought about by high shear rates during manufacture due to melt processing. When the CNC content is increased, a significant increase in the agglomerate fraction is detected. These observations support the assumption of good dispersion at very small contents of nanocellulose.

Thermogravimetric Analysis (TGA)

The neat PHB injection molded samples as well as the bionanocomposites with 1 and 3 wt% nanocellulose are analyzed by means of TGA. The TGA curves of the samples in dependence on the heating temperature as well as the corresponding derivative curves (DTG) are shown in Fig. 2. Neat PHB shows a degradation onset at 281 °C, which is a similar value to the reported by the bibliography [29]. The higher thermal stability of CNC has already been demonstrated in other sources with thermal degradation above 320 °C [30, 31]. As can be seen in Fig. 2a, the addition of crystalline nanocellulose to PHB matrix does not decrease the onset temperature with increasing amounts of CNC as occurs in Srithep et al. [32], who have reported an onset degradation temperature decrease when nanofibrillated cellulose (NFC) is added to PHBV matrix and they are processed by melt compounding. They attributed this phenomenon to residual moisture. Similarly, Panaitescu et al. [29] reported a diminution of onset and maximum degradation temperatures in biocomposites prepared by the addition of bacterial cellulose

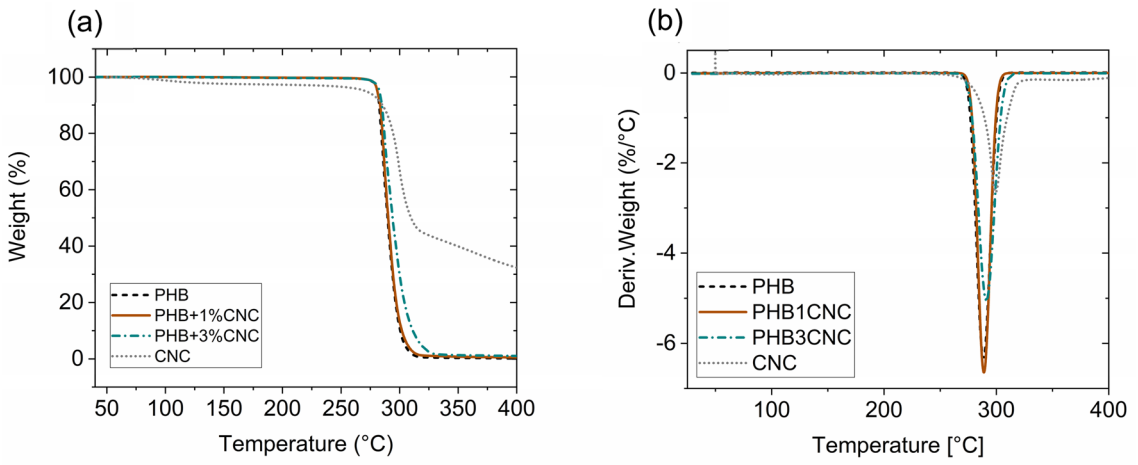

Fig. 2 Thermal analysis of pure CNC, neat PHB and its bionanocomposites: **a** TGA and **b** DTG curve

(BC) nanofibers to PHB/PHHO blends using solution casting methodology. They attributed this to the presence of bonded water in BC nanofibers, which is released at higher temperatures and may also favors the degradation of PHB. In view of the results obtained, the previous drying step of the materials seems to prevent the loss of thermal resistance of the bionanocomposites prepared in this work. Seoane et al. [31] have found a positive effect of nanocellulose reinforcement in the thermal degradation of PHB based on nanocomposite films prepared by solution casting with a previous sonication step. They have seen an slightly increase in the onset temperature values in PHB matrix with the addition of CNC. They manifest that this increase is in accordance to the greater stability of CNC as regards to PHB. In the present work, the same phenomenon is observed as can be seen in Fig. 2a.

In DTG curves (Fig. 2b) are observed that the maximum degradation temperatures were shifted to higher values with increasing CNC contents. Martínez-Sanz et al. [33] reported that the degradation onset and maximum degradation temperature were shifted to higher temperatures for a low loading of 1 wt% bacterial cellulose nanowhiskers (BCNW) in PHBV matrix when the composites are prepared by solution casting. However, further increases in nanofiller loading resulted in decreased thermal resistance, which is attributed to the poor dispersion and agglomeration of cellulose nanowhiskers with increasing particle content in the matrix. They attribute this to the reduction of hydroxyl groups available in the nanocrystals surface to form hydrogen bonds with the polymeric matrix and thus, the thermal stability provided by the addition of BCNW can be restricted for higher contents. Yu et al. [17] reported a gradually increase on maximum degradation temperatures with increasing contents of cellulose nanocrystalline (CNC) in PHBV matrix, prepared by solution casting, when a previous step of exposition to ultrasonic irradiation is included in the procedure. They attribute this to the intermolecular hydrogen bonding interactions between CNC and PHBV on the one hand and the homogeneous dispersion of nanofiller. In this work, the previous step of ultrasonic stabilization of CNC water suspension to the melting processing seems avoid the agglomeration and favors the good dispersion of the lower contents of CNC in PHB matrix, which can lead to think about the existence of CNC-matrix interactions, avoiding the diminution of thermal stability of bionanocomposites prepared.

Differential Scanning Calorimetry (DSC)

The differential scanning calorimetry of the bionanocomposites provides information on their thermal properties and crystallization behavior. In Fig. 3 the heat flow in dependence on the temperature of PHB and its bionanocomposites with 1 and 3 wt% nanocellulose is presented for a cooling rate of 30 °C min^{-1}. A relatively high cooling rate is chosen in order to better understand the behavior of the polymer melt during common industrial processing techniques such as injection molding. It can be observed that the crystallization temperature of PHB (T_c), reported in Table 1, increases by the addition of CNC, which is ascribed to a nucleating effect of these nanofillers. This assumption is supported by the findings of several authors. Ten et al. [34] and Yu et al. [17] described a nucleating effect of cellulose nanowhiskers and CNC, respectively, on PHBV prepared by solution casting, which reduce the energy barrier to form PHBV nuclei. Seoane et al. [31] related the displacement of PHB crystallization peak to higher temperatures with the incorporation of CNC, observed in PHB films made by solution casting, to a nucleating agent effect of nanofiller in the PHB matrix. Scalioni et al. [7] related also this increase of T_c values with a heterogeneous nucleation mechanism of PHB

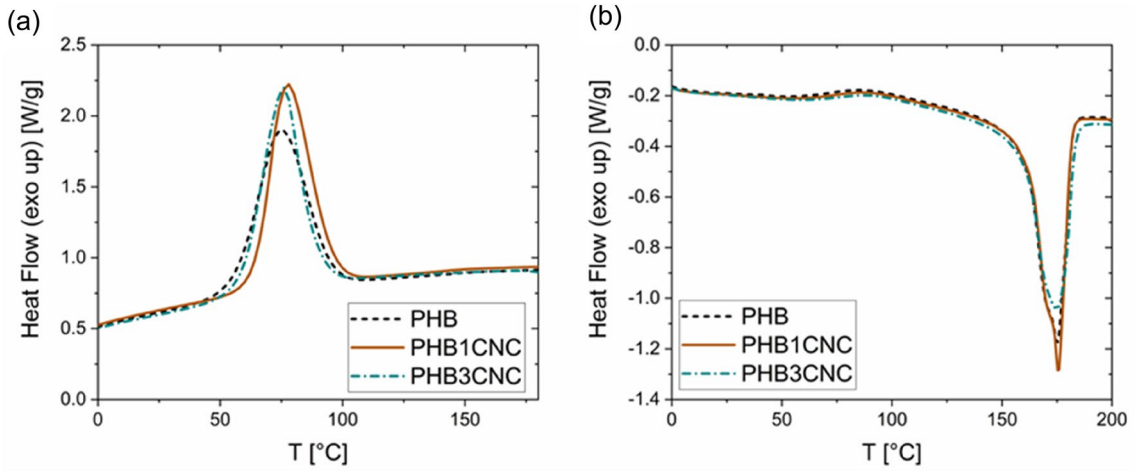

Fig. 3 Crystallization temperature of PHB and its biocomposites during DSC cooling scan (**a**) and melting behavior of PHB and its bionanocomposites during DSC second heating scan (**b**)

Table 1 Results from DSC cooling and subsequent heating scan: crystallization temperature Tc, |Tc(onset) − Tc|, melting temperature Tm and degree of crystallinity χc, as well as the crystallinity fraction, by using Ruland Vonk method, and average crystallite size, by using Scherrer´s equitation, in main planes (020) and (110) of PHB and the bionanocomposites calculated by using XRD

Material	T_c [°C]	$\lvert T_{c(onset)} - T_c \rvert$ [°C]	T_m [°C]	χ_c [%] *DSC*	χ_c [%] *XRD*	$D_{(0\,2\,0)}$ [nm]	$D_{(1\,1\,0)}$ [nm]
PHB	74.0	19.7	174.1	56.6	43.9	22.1	20.9
PHB1CNC	78.0	15.1	174.5	59.8	46.9	18.1	19.1
PHB3CNC	76.0	17.1	174.1	58.3	47.0	19.8	18.9

based biocomposites melting processed by using a plasticizer agent, where the fibers act as a nucleating agent. This phenomenon is related to an enhancement in the chain diffusion by the presence of the fibers which increases the crystallization rate. In the present study, this nucleating effect of CNC on PHB matrix as well as a higher crystallization rate were also observed in these melting processed bionanocomposites with a previous sonication step, to ensure the good dispersion of CNC in PHB matrix, but in absence of plasticizer agents. These findings were also observed and corroborated by POM analysis as will be described in the section "Polarized Optical Microscopy (POM)". Moreover, the parameter $T_{c(onset)} - T_c$ was determined and reported in Table 1, being a measure for the overall crystallization rate: the smaller this parameter, the higher the crystallization rate [17]. For CNC containing bionanocomposites the parameter $T_{c(onset)} - T_c$ decreases compared to neat PHB, with the highest acceleration of the crystallization process for 1 wt% CNC content. This finding further supports the hypothesis of increased nucleation caused by CNC.

The melting temperature of neat PHB derived from Fig. 3 is reported in Table 1 and it is in the same range as published by Scalioni et al. [7] who reported a melting temperature of 177 °C. The analysis of the melting behavior for the bionanocomposite materials reveals no influence of the addition of crystalline nanocellulose on the melting temperature of PHB. This matter was further investigated by polarized optical microscopy analysis and their results will be described in the below section "Polarized Optical Microscopy (POM)"

Table 1 summarizes the data characterizing the crystallization behavior of the biopolymer and bionanocomposites. The calculated degrees of crystallinity show that the addition of CNC leads to an increased crystallinity, with a maximum for 1 wt% of nanocellulose contents. This corresponds with the crystallization behavior observed during cooling, displaying the highest crystallization peak temperature for bionanocomposites with 1 wt% CNC. A possible explanation could be a better dispersion of the smaller weight fraction of 1 wt% CNC in PHB, leading to a larger interface between CNC and PHB and, thus, favoring the CNC's nucleating effect [33]. Often, higher weight fractions of nanoparticles are more difficult to disperse, which could reduce their effect on the polymer matrix. This issue was investigated and corroborated by the transmission electron microscopy analysis, which results were presented the section "Transmission electron microscopy (TEM)" of this article.

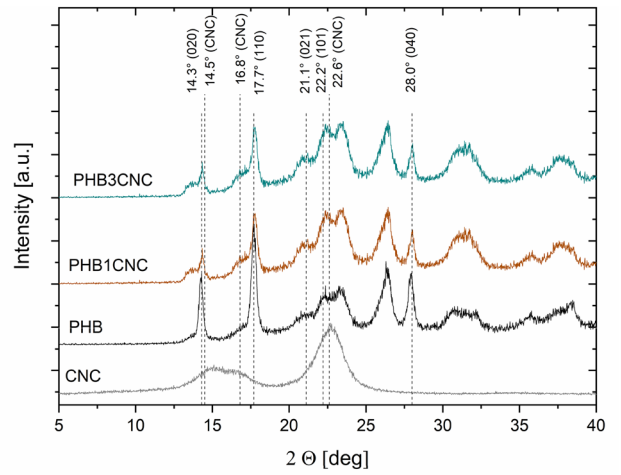

Fig. 4 X-ray diffraction pattern of the pure CNC, neat PHB and PHB with 1 and 3 wt% CNC

X-ray Diffraction

The physical properties of the bionanocomposites depend on the crystallinity behavior of PHB, so, the influence of the incorporation of cellulose particles on this behavior was investigated using XRD. In the Fig. 4 are shown the obtained diffractograms for the neat PHB and the bionanocomposites performed at room temperature. All of them showed a diffraction pattern corresponding to an orthorhombic unit cell typical of α-form of PHB, which is constituted by two left-handed helical molecules packed together in an antiparallel orientation, with two main peaks at 2θ values of 14.3°, 17.7° assigned to (020) and (110) planes, respectively; three weaker and broader peaks at 21.1° (021), 22.2° (101) and 23.2° (111), two well-defined and intense peaks at 26.3° (121) and 28.0° (040) and, finally, some weaker peaks observed at 31.3° (002), 32.2° (200), 35.8° (201) and 38.5° (122) [7, 29].

The diffractogram of cellulose nanocrystalline is well known and consists of two weak peaks appearing at 2θ values of 14.5°, 16.8° and the main peak at 22.6° of considerably higher intensity [30]. As occurs to other authors, the peaks at lower angles cannot be observed in the bionanocomposite diffractograms and the 22.6° peak appears convoluted with the contribution of PHB peaks, leading to a widening and an intensification of the peaks in this region [17]. Since the location of the peaks for the PHB matrix remains the same for the most part, no change in this crystal structure is assumed, α-crystals are predominant in the bionanocomposites.

Furthermore, it is found that the intensities of main peaks at 2θ values of 14.3° and 17.7° diminish when CNC is incorporated into neat PHB. This fits with the assumption that the CNC acts as an efficient nucleation agent, promoting the crystallization rate.

The calculations of the crystallinity of the spectra and the crystallite size of the two principal planes, (020) and the (110) are shown in Table 1. An increase in crystallinity by the addition of CNC from 43% to about 47% is consistent with the DSC observations. Furthermore, a broadening of the peaks is observed by incorporating CNC, corresponding to a reduction of the crystal size calculated by Scherrer's equations [36, 37]. These results support the DSC assumption that CNCs act as nucleating agents in PHB [24, 38].

Polarized Optical Microscopy (POM)

Further qualitative investigations of the crystallization behavior of the bionanocomposites are performed by polarized optical microscopy. Figure 5 shows images of PHB and its bionanocomposites at different temperatures when cooling down the materials from the melt state at 210 °C to room temperature. The CNC can be observed dispersed in the molten state of the bionanocomposites in the image at 210 °C. PHB spherulites with characteristic banding and Maltese cross could be clearly seen along the cooling process. Moreover, the neat PHB and its bionanocomposites show similar morphological evolution with temperature. As already concluded from the heating scan of DSC analysis and XRD analysis, there is no hint in the POM images of a change of crystal morphology due to CNC.

By comparing the images at different temperatures along the cooling process, the addition of nanocellulose causes that the crystallization starts at higher temperatures, more crystals are formed compared to neat PHB and crystallization is completed at lower temperatures. Furthermore, a reduction of the crystal diameters is noted. This acceleration of the crystallization can be attributed to the nucleating effect of CNC and is consistent with the results from the DSC cooling scan and Table 1.

Finally, at room temperature, the number of PHB spherulites in neat PHB was small and their size was relatively big because the spherulites had large space to grow before impinging on each other. With the addition of CNC, the number of PHB spherulites increased and consequently their size was in general reduced as occurred to Yu et al. [39], who observed smaller spherulites after the addition of CNC to PHBV due to the radial growth of numerous spherulites based on CNCs nuclei would cease once the surfaces of PHBV spherulites contacted each other. Ten et al. [40] observed that the addition of cellulose nanowhiskers (CNW) to PHBV lead to an increment in the number of spherulites and a reduction of their size, which was attributed to the nucleation effect of CNW. The evaluation of the polarized light microscope images therefore completely confirms the DSC and XRD measurements.

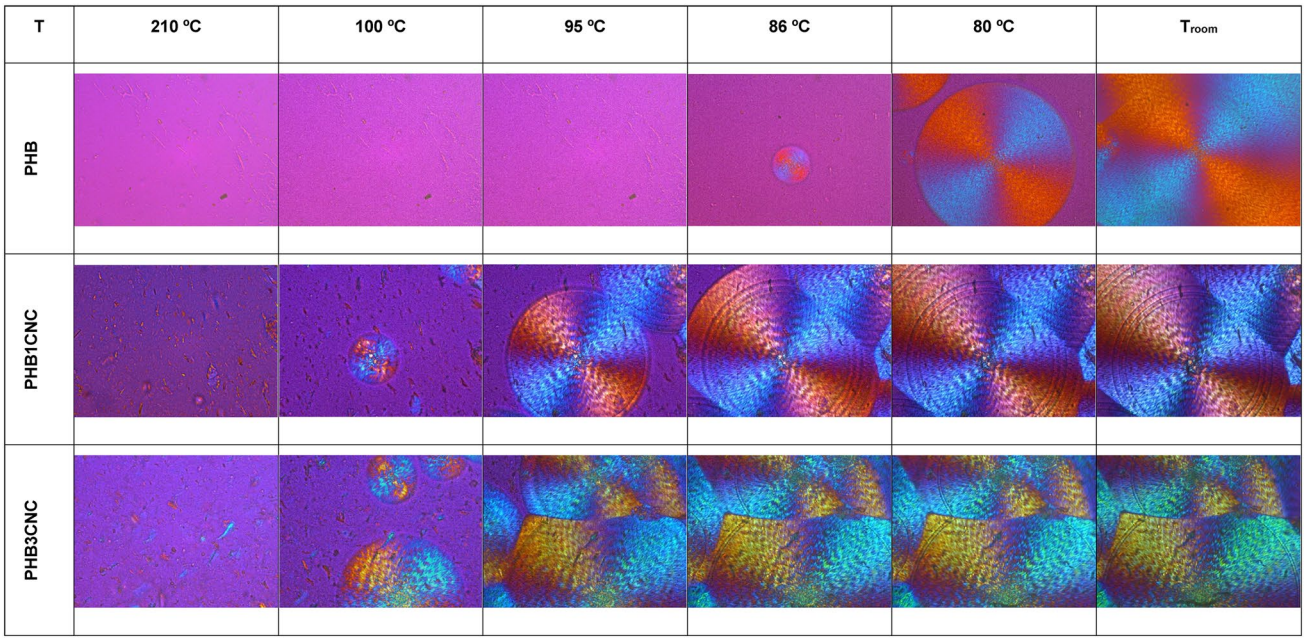

Fig. 5 POM images of PHB and its bionanocomposites when cooling the materials down from 210 °C to room temperature

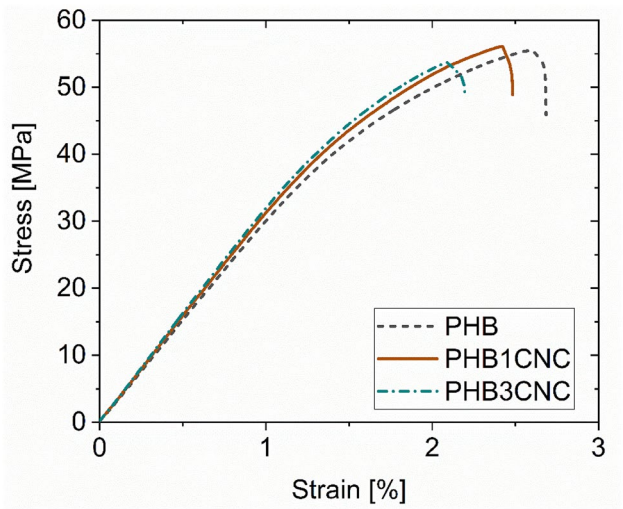

Fig. 6 Stress-strain diagrams of PHB and its bionanocomposites containing 1 and 3 wt% of nanocellulose

Three-Point Bending Test

The injection molded samples were tested in three-point bending configuration in order to determine their modulus, bending strength and bending elongation. Figure 6 shows representative stress-strain diagrams of the neat PHB and its bionanocomposites with 1 and 3 wt% CNC. Table 2 summarizes the mean values and standard deviations of the three-point bending test.

Table 2 Mean values and standard deviation of bending modulus E, bending strength σ and bending elongation ε

Material	E [MPa]	σ_m [MPa]	ε_m [%]
PHB	3080 ± 78	55 ± 2	2.5 ± 0.2
PHB1CNC	3214 ± 68	57 ± 1	2.4 ± 0.1
PHB3CNC	3263 ± 61	54 ± 1	2.1 ± 0.1

The results of the three-point bending test reveal that the addition of nanocellulose to poly(hydroxybutyrate) leads to an increase of the material's stiffness (modulus), the increase being higher for higher weight contents of CNC, which indicates the reinforcing effect of CNC in PHB bionanocomposites. Probably, the previous step of CNC dispersion made before the processing of the bionanocomposites leaded to a better dispersion of CNC in the PHB matrix, favoring the good interfacial adhesion and the reinforcing effect. For the bending strength, there is only a slight increase after addition of 1 wt% CNC. No effect on the bending strength can be observed for the higher CNC content, probably ascribing to nanocellulose agglomeration observed by TEM imaging. These created regions of stress concentration that can initiate or propagate more cracks, which can generate images as the obtained by SEM imaging for bionanocomposites with 3 wt% CNC in the section "Scanning electron microscopy (SEM)" below. Concerning the maximum elongation, a detrimental effect is observed with increasing amount of nanocellulose, maybe due to an increase in the rigidity of the interphase CNC-PHB, as will be corroborated by DMA

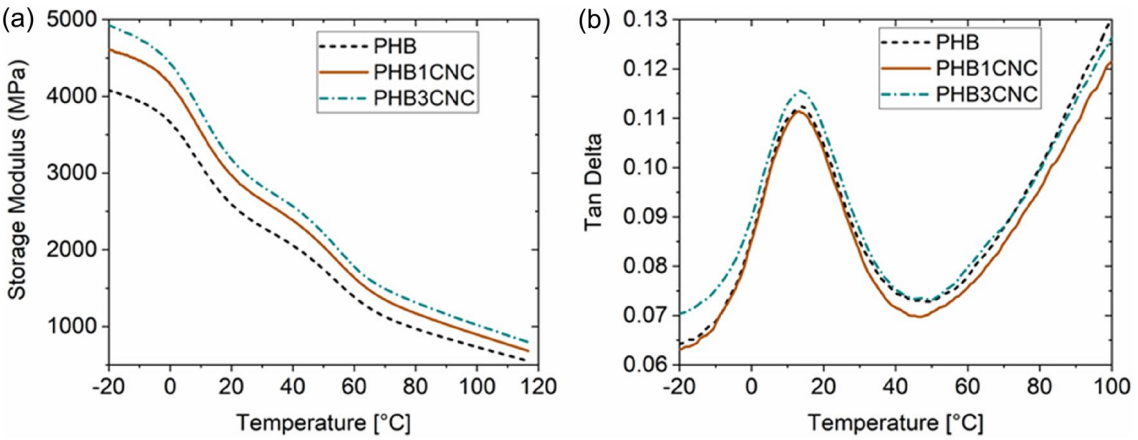

Fig. 7 Evolution (at a frequency of 1 Hz) of storage modulus and loss factor (Tan Delta) with temperature for neat PHB and its bionanocomposites

in the next section. Moreover, it is believed that all three effects, the improvement of stiffness and strength as well as the decrease of the elongation can be ascribed to the increase in crystallinity caused by the cellulose, which was previously observed by DSC and XRD analysis. While the higher crystallinity has a reinforcing effect on the modulus and strength, it simultaneously leads to a higher brittleness, which affects the elongation.

Comparing all bending properties, it can be concluded that the optimum material behavior is achieved for the bionanocomposites with 1 wt% CNC, as occurred to other authors as Dasan et al. [41], who reported a similar tendency for the reinforcing effect of nanocrystalline cellulose in a blend of PLA and PHBV. They obtained better bending properties for smaller amount of CNC with a maximum of the mechanical properties at even lower fractions of 0.25 wt% of CNC. Jun et al. [6] also reported the reinforcing effect of CNC in PHBV matrix and they declared that the bionanocomposite with the 1 wt% of CNC showed the optimum tensile elongation at break of all the bionanocomposites analyzed.

Dynamic Mechanical Analysis (DMA)

The effects of CNC in the dynamic mechanical properties of the bionanocomposites was examined by DMA. Storage modulus (*E'*) and *Tan δ* values vs temperature curves were represented in Fig. 7.

The reinforcing action of CNC in the PHB matrix observed during the bending test of the bionanocomposites is corroborated by DMA analysis as the storage modulus increased during the whole temperature range with the addition of CNC, as occurred in the bending test of bionanocomposites performed at room temperature.

With respect to the *Tan δ* curves, the addition of CNC to the PHB matrix hardly affects to the glass transition values of bionanocomposites with lower CNC content and therefore, to the polymer chains mobility in this case. The *Tg* value obtained for bionanocomposite with 3 wt% CNC is slightly higher, indicating a slight restriction of the mobility of the amorphous chains close to the crystals due to the addition of CNC to the matrix. This limitation of chain mobility into the matrix can be due to the restraint of CNC in PHB spherulites, whose size decreased after the addition of CNC as was reported from the results of POM images described above. The aggregates seen by SEM and TEM imaging could be responsible for this restriction. Several authors have reported this increment in the glass transition temperature values when cellulosic derivates are added to PHA matrixes [32, 34]. In this case, this phenomenon was avoided with the processing method used and, as was concluded in the previous analysis of the results from the bending test made, the optimum mechanical behavior was achieved for the bionanocomposites with 1 wt% CNC, which show a higher storage modulus without increasing the glass transition temperature.

Scanning Electron Microscopy (SEM)

Cryo-fractured surfaces of neat PHB and its bionanocomposites after being made the bending test were analyzed by SEM at 2000 times magnification (see Fig. 8).

For the neat PHB (Fig. 8a), there can be observed a relatively smooth fracture surface containing some impurities, which, as described above, suggest bacterial residues (marked with a white circle in (a)). The bionanocomposite containing 1 wt% CNC (Fig. 8b) showed an even dispersion and distribution of the nanocellulose over the whole material. By contrast, the roughness of the cryo-fractured images increased with the nanofiller loading. The fracture surface of bionanocomposites containing 3 wt% CNC (Fig. 8c) displays some nanoparticle agglomerates, marked with a black circle,

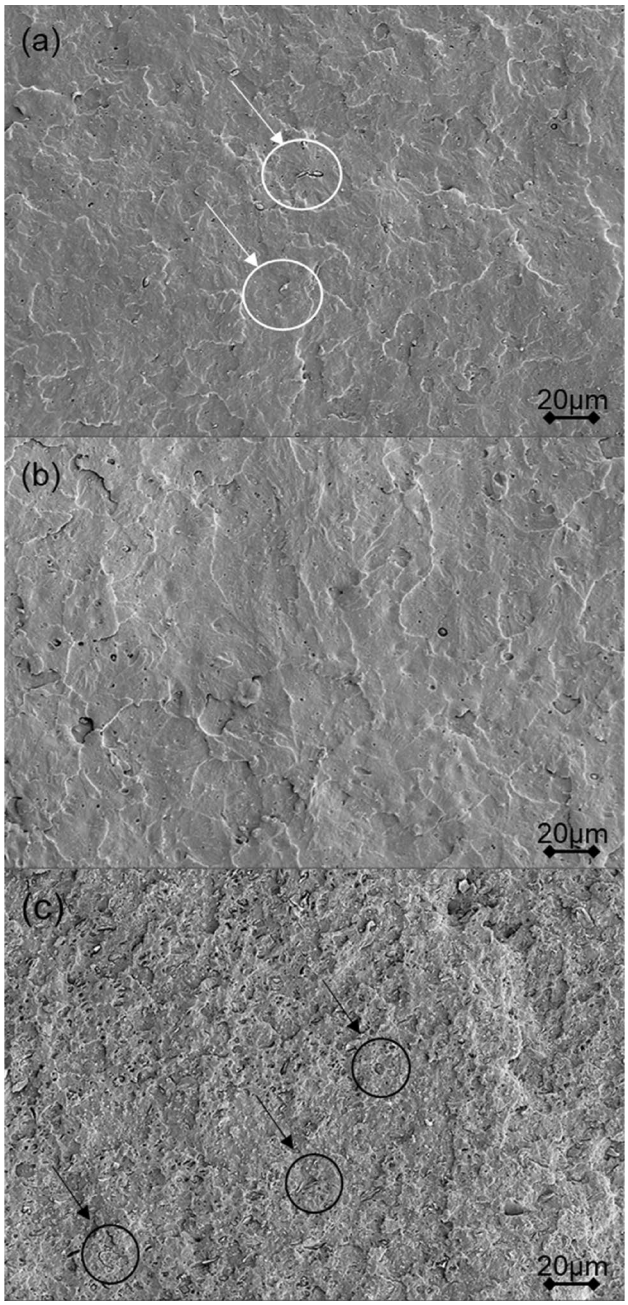

Fig. 8 SEM images of the fracture surface of neat PHB (**a**), PHB with 1 wt% CNC (**b**) and PHB with 3 wt% CNC. In (**a**) neat PHB, impurities are marked with white circles. In **c** PHB with 3 wt% CNC, agglomerates of CNC are marked with black circles

and a much rougher surface with higher voids than the other materials as occurs to other authors. Martínez-Sanz et al. [33] have also described a better dispersion of lower bacterial cellulose nanowhiskers (BCNW) contents in a PHBV matrix, where some BCNW agglomerates are observed for 3 wt% BCNW content. The inferior dispersion of nanocellulose in these samples could explain the lower benefit of 3 wt% CNC on the crystallization, nucleation, and tensile strength of PHB compared to 1 wt% CNC, as described above. With respect to the higher amount of voids observed in the bionanocomposite with 3 wt% CNC, Angelini et al. [13] have attributed this phenomenon to the inhibited diffusion of the polymer melt within the aggregate lignin particles lumps in PHB matrix. The presence of agglomerates leads to the appearance of debonding zones between the filler and the polymer matrix, which favors the generation of flaws affecting to the mechanical response of the bionanocomposite as was described in sections "Three-point bending test" and "Dynamic mechanical analysis (DMA)" and probably to their moisture absorption as well as to the barrier properties, as will be described in sections "Moisture absorption test" and "Barrier properties", respectively.

Table 3 Moisture absorption after exposure of 1056 h to distilled water

Sample	Moisture absorption after 1056 h
PHB	0.40 ± 0.04%
PHB1CNC	0.10 ± 0.02%
PHB3CNC	0.60 ± 0.02%

Moisture Absorption Test

The moisture absorption is an important property for food packaging systems, that the materials should avoid or, at least, minimizing the water absorption to achieve the desired food protection. In order to study this issue, the moisture absorption rate was obtained for the neat PHB and the bionanocomposites. Dried samples of neat PHB polymer and its bionanocomposites were stored for 1056 h in distilled water. The samples were weighed at the start of the analysis as well as at different times in order to calculate the moisture absorption values from Eq. (4). The moisture absorption curves were obtained by representing these values against the time. A quick increment of moisture absorption values was observed during the early hours of exposure until reaching an approximately stable value. The moisture absorption values corresponding to the end of the exposition were presented in Table 3. For all the materials relatively low moisture absorption of less than 1 wt% was measured. By contrast, the addition of nanofillers in general is reported to lead to an increase in moisture absorption up to several percent of the weight [20, 28, 43]. Montanheiro et al. [43] and Valente et al. [44] also describe lower moisture absorption for the neat PHA than for the prepared composites. However, this high weight gains due to moisture absorption, which may limit the material's applications, was not observed in the nanocellulose-reinforced bionanocomposites investigated in the present study.

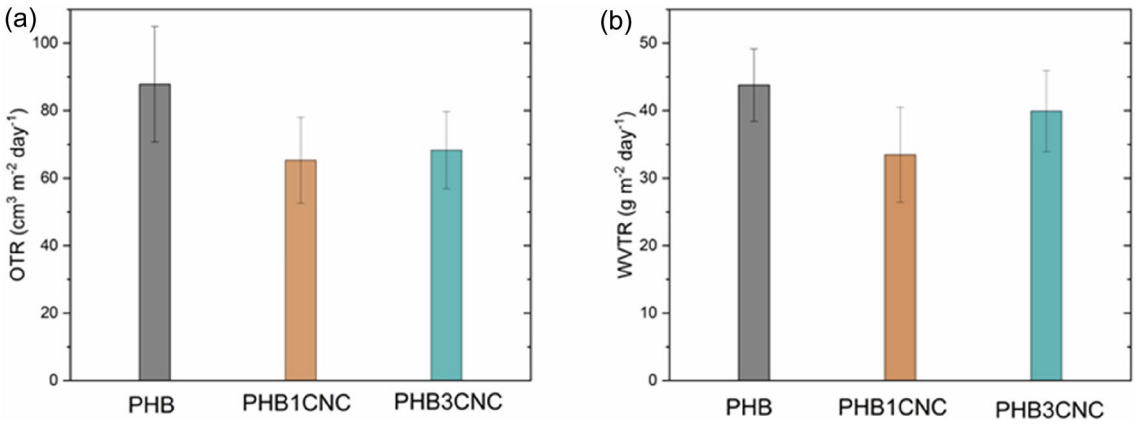

Fig. 9 Oxygen transmission rate (OTR) and water vapor transmission rate (WVTR) for neat PHB and its bionanocomposites

The decrease in moisture absorption capacity for bionanocomposites with lower CNC contents can be attributed to the homogeneous dispersion, which could be favored by the use of sonification during the processing step, leading to a good interaction of the filler with the matrix. However, when the filler content in the matrix increases, the formation of aggregates generates voids, as can be seen in the SEM images, which allows water molecules to pass through the matrix. This added to the higher hydrophilicity of CNC versus PHB, may explain why a higher CNC content generates an increase in moisture absorption capacity. As occurs with the mechanical properties, the bionanocomposite with an amount of 1 wt% of CNC shows the more desirable behavior in relation to the moisture absorption capacity. Thus, compared with pure PHB and PHB with 3 wt% CNC, this bionanocomposite has more suitable mechanical properties and higher moisture absorption resistance, which is essential for use in the packaging industry.

Barrier Properties

For the application as packaging material, gas barrier properties are crucial in addition to sufficient mechanical properties and moisture absorption. The oxygen and water vapor transmission rate of both, PHB and bionanocomposite films, were collected. The initial transmission rate values increased progressively in the first hours of the test until reaching a constant value after approximately 5 h in all cases. The analysis were prolonged until the 25 h to ensure the steady state was reached. In the Fig. 9 are represented the average of the transmission rate values obtained in this steady state of the transmission rate curves. Both nanocellulose reinforced bionanocomposites showed a reduction in oxygen transmission rate as well as water vapor transmission rate, however the incorporation of 1 wt% CNC had a greater effect on barrier properties than in the bionanocomposites reinforced with 3 wt%. The values decreased in oxygen transmission and water vapor transmission from 87.8 cm^3 m^{-2} day^{-1} and 43.8 g m^{-2} day^{-1} to 65.3 cm^3 m^{-2} day^{-1} and 33.5 g m^{-2} day^{-1} for PHB with 1 wt% CNC, respectively. Increasing the cellulose content to 3 wt% increased the values again to 68.3 cm^3 m^{-2} day^{-1} and 40.0 g m^{-2} day^{-1}. The OTR and WVTR values were lower to those determined by Malmir et al. [45] for PHB with CNC produced by solvent casting, so, the processing method used in this work lead to materials with better permeability characteristics, which is very interesting as this procedure is clearly closer to the industrial scale processing than the solving casting. Qasim et al. [46] also studied PHB reinforced with cellulose and also determined higher WVTR and OTR values, but they found similar trends for small contents of the filler.

Permeability depends on several steps: First, adsorption of the permeant to the film surface occurs, followed by entry and diffusion towards the side with lower concentration, and then release into the environment, desorption. Due to the many times higher free volume in the amorphous phase, the permeation is mainly determined by the ratio between amorphous and crystalline fractions. Furthermore, the permeability is influenced by the size and polarity of the permeant, which lead to the varying degrees of improvement in gas barrier properties to water vapor molecules compared to oxygen molecules [47]. The improve in gas barrier properties was accompanied by the previously observed higher crystallinity as well as the nanocellulose content of the bionanocomposites. Consequently, the nucleating effect of the CNC leads to an increased crystallinity which is similar to a larger non-permeable area [46]. Furthermore, the incorporation of the non-permeable CNC into the matrix leads to a tortuous pathway of the molecules [48]. Some studies [49, 50] additionally assume the formation of networks between the CNC crystals (transient percolation network) as well as the PHB in the CNC (intercalation network) via hydrogen

bonds, which enhance this effect. However, the TEM images given no indication of a network in this composite. In contrast, the formation of agglomerates and defects, like voids due to the different polarity of the polar PHB matrix and the non-polar CNC, had an increasing influence on the permeability and counteracts the above-mentioned effects. These impacts increased with increasing particle fraction and in turn leaded to a slightly lower OTR and WVTR at 3 wt% CNC [49].

Conclusion

In this study, the properties and the behavior under environmental conditions of polyhydroxybutyrate bionanocomposites melt processed by preindustrial methods and reinforced with 1 wt% and 3 wt% of biobased crystalline nanocellulose were analyzed in order to determinate their applicability on the packaging industry. A previous step of ultrasonication during the processing allowed to obtain materials with a good dispersion of the lower cellulose contents however, at higher CNC contents, the formation of aggregates was observed, which prevented the improvement of the tested properties. In all cases, the degree of crystallinity was higher with the addition of CNC particles, which acted as nucleating agent, inducing heterogeneous crystallization, leading to an acceleration of PHB crystallization from the polymer melt and resulting in more and smaller PHB crystals, as was confirmed by POM image analysis over the entire temperature range of the crystallization process. A reinforcing effect of CNC was related to the enhancement of stiffness and strength observed in the bionanocomposites and to the increase in the storage modulus throughout the temperature range. However, the T_g value increased for this material, indicating a limitation in the chain mobility into the matrix due to the presence of CNC agglomerates, especially for higher CNC contents. The same tendency as for the other analyses was shown related to the moisture absorption capacity and the gas barrier properties, bionanocomposites with 1 wt% CNC exhibit a decreased moisture absorption and also better barrier properties compared to neat PHB, while the positive impact diminished somewhat for materials with 3 wt% CNC. Therefore, it can be concluded that the completely green bionanocomposites with a 1 wt% CNC could be a good alternative for different applications in the packaging industry in which it is necessary moisture absorption resistance and good gas barrier properties.

Acknowledgements The authors would like to thank Melodea Ltd., Israel, for providing samples of cellulose nanocrystal water suspension.

Author Contributions All authors contributed to the study conception and design. Material preparation, data collection and analysis were performed by AS. The first draft of the manuscript was written by AS and all authors commented on previous versions of the manuscript.

Funding Open Access funding provided thanks to the CRUE-CSIC agreement with Springer Nature. This work was partially supported by Xunta de Galicia Government and FEDER: program of consolidation and structuring competitive research units [Grant Number: ED-431 C 2019/1]. Funding for open access charge was given by Universidade da Coruña/CISUG.

Data Availability The datasets generated during the current study are available from the corresponding author on reasonable request.

Declarations

Competing Interests The authors declare no competing interests.

References

1. Nanda S, Patra BR, Patel R, Bakos J, Dalai AK (2022) Innovations in applications and prospects of bioplastics and biopolymers: a review. Environ Chem Lett 20:379–395
2. Dicker MPM, Duckworth PF, Baker AB, Francois G, Hazzard MK, Weaver PM (2014) Green composites: a review of material attributes and complementary applications. Compos Part A Appl Sci Manuf 56:280–289
3. Pickering KL, Efendy MGA, Le TM (2016) A review of recent developments in natural fibre composites and their mechanical performance. Compos Part A Appl Sci Manuf 83:98–112
4. Vilaplana F, Strömberg E, Karlsson S (2010) Environmental and resource aspects of sustainable biocomposites. Polym Degrad Stab 95:2147–2161
5. Evstatiev M, Simeonova S, Friedrich K, Pei XQ, Formanek P (2013) MFC-structured biodegradable poly(l-lactide)/poly(butylene adipate-co-terephatalate) blends with improved mechanical and barrier properties. J Mater Sci 48:6312–6330
6. Jun D, Guomin Z, Mingzhu P, Leilei Z, Dagang L, Rui Z (2017) Crystallization and mechanical properties of reinforced PHBV composites using melt compounding: effect of CNCs and CNFs. Carbohydr Polym 168:255–262
7. Scalioni LV, Gutiérrez MC, Felisberti MI (2017) Green composites of poly(3-hydroxybutyrate) and curaua fibers: morphology and physical, thermal, and mechanical properties. J Appl Polym Sci 134:1–13
8. Kennouche S, Le Moigne N, Kaci M, Quantin JC, Caro-Bretelle AS, Delaite C, Lopez-Cuesta JM (2016) Morphological characterization and thermal properties of compatibilized poly(3-hydroxybutyrate-co-3-hydroxyvalerate) (PHBV)/poly(butylene succinate) (PBS)/halloysite ternary nanocomposites. Eur Polym J 75:142–162

9. Philip S, Keshavarz T, Roy I (2008) Review polyhydroxyalkanoates: biodegradable polymers with a range of applications. J Chem Technol Biotechnol 83:1163–1169
10. Kumar M, Rathour R, Singh R, Sun Y, Pandey A, Gnansounou E, Lin KYA, Tsang SCW, Thakur IS (2020) Bacterial polyhydroxyalkanoates: Opportunities, challenges, and prospects. J Clean Prod 263:121500
11. Hempel F, Bozarth AS, Lindenkamp N, Klingl A, Zauner S, Linne U, Steinbüchel A, Maier UG (2011) Microalgae as bioreactors for bioplastic production. Microb Cell Fact 10:2–7
12. Lee CH, Sapuan SM, Ilyas RA, Lee SH, Khalina A (2020). Advanced processing, properties, and applications of starch and other bio-based polymers. Elsevier Inc.
13. Angelini S, Cerruti P, Immirzi B, Santagata G, Scarinzi G, Malinconico M (2014) From biowaste to bioresource: effect of a lignocellulosic filler on the properties of poly(3-hydroxybutyrate). Int J Biol Macromol 71:163–173
14. Tan KW, Heo SK, Foo ML, Chew IM, Yoo C (2019) An insight into nanocellulose as soft condensed matter: challenge and future prospective toward environmental sustainability. Sci Total Environ 650:1309–1326
15. Isogai A (2021) Emerging Nanocellulose Technologies: recent developments. Adv Mater 33:2000630
16. Mariano M, El Kissi N, Dufresne A (2014) Cellulose nanocrystals and related nanocomposites: review of some properties and challenges. J Polym Sci Part B Polym Phys 52:791–806
17. Yu HY, Qin ZY, Liu L, Yang XG, Zhou Y, Yao JM (2013) Comparison of the reinforcing effects for cellulose nanocrystals obtained by sulfuric and hydrochloric acid hydrolysis on the mechanical and thermal properties of bacterial polyester. Compos Sci Technol 87:22–28
18. Omran AAB, Mohammed AABA, Sapuan SM, Ilyas RA, Asyraf MRM, Koloor SSR, Petrú M (2021) Micro- and nanocellulose in polymer composite materials: a review. Polym (Basel) 13:1–30
19. Panaitescu DM, Nicolae CA, Gabor AR, Trusca R (2020) Thermal and mechanical properties of poly(3-hydroxybutyrate) reinforced with cellulose fibers from wood waste. Ind Crops Prod 145:112071
20. Arrieta MP, Peponi L, López D, López J, Kenny JM (2017) In: Grumezescu AM (ed) Food Packaging. Elsevier Inc., Romania
21. Lee J, Park HJ, Moon M, Lee JS, Min K (2021) Recent progress and challenges in microbial polyhydroxybutyrate (PHB) production from CO2 as a sustainable feedstock: a state-of-the-art review. Bioresour Technol 339:125616
22. Dhar P, Bhardwaj U, Kumar A, Katiyar V (2017) Investigations on rheological and mechanical behavior of poly(3-hydroxybutyrate)/cellulose nanocrystal based nanobiocomposites. Polym Compos 38:E392-401
23. Garcia-Garcia D, Lopez-Martinez J, Balart R, Strömberg E, Moriana R (2018) Reinforcing capability of cellulose nanocrystals obtained from pine cones in a biodegradable poly(3-hydroxybutyrate)/poly(ε-caprolactone) (PHB/PCL) thermoplastic blend. Eur Polym J 104:10–18
24. Seoane IT, Luzi F, Puglia D, Cyras VP, Manfredi LB (2018) Enhancement of paperboard performance as packaging material by layering with plasticized polyhydroxybutyrate/nanocellulose coatings. J Appl Polym Sci 135:1–11
25. Barham PJ, Keller A, Otun EL, Holmes PA (1984) Crystallization and morphology of a bacterial thermoplastic: poly-3-hydroxybutyrate. J Mater Sci 19:2781–2794
26. Vonk GC (1973) Computerization of Ruland's X-ray method for determination of the crystallinity in polymers. J Appl Crystallogr 6:148–152
27. Langford JI, Wilson AJC (1978) Seherrer after sixty years: a survey and some new results in the determination of crystallite size. J Appl Crystallogr 11:102–113
28. Bittmann B, Bouza R, Barral L, Bellas R, Cid A (2018) Effect of environmental factors on poly(3-hydroxybutyrate-co – 3-hydroxyvalerate)/Poly(butylene adipate-co-terephthalate)/ montmorillonite nanocomposites with antimicrobial agents. Polym Compos 39:915–923
29. Panaitescu DM, Frone AN, Chiulan I, Nicolae CA, Trusca R, Ghiurea M, Gabor AR, Mihailescu M, Casarica A, Lupescu I (2018) Role of bacterial cellulose and poly (3-hydroxyhexanoate-co-3-hydroxyoctanoate) in poly (3-hydroxybutyrate) blends and composites. Cellulose 25:5569–5591
30. Montero B, Rico M, Barral L, Bouza R, López J, Schmidt A, Bittmann-Hennes B (2021) Preparation and characterization of bionanocomposite films based on wheat starch and reinforced with cellulose nanocrystals. Cellulose 28:7781–7793
31. Seoane IT, Cerrutti P, Vazquez A, Manfredi LB, Cyras VP (2017) Polyhydroxybutyrate-based nanocomposites with cellulose nanocrystals and bacterial cellulose. J Polym Environ 25:586–598
32. Srithep Y, Ellingham T, Peng J, Sabo R, Clemons C, Turng LS, Pilla S (2013) Melt compounding of poly (3-hydroxybutyrate-co-3-hydroxyvalerate)/ nanofibrillated cellulose nanocomposites. Polym Degrad Stab 98:1439–1449
33. Martínez-Sanz M, Villano M, Oliveira C, Albuquerque MGE, Majone M, Reis M, López-Rubio A, Lagarón JM (2014) Characterization of polyhydroxyalkanoates synthesized from microbial mixed cultures and of their nanobiocomposites with bacterial cellulose nanowhiskers. N Biotechnol 31:364–376
34. Ten E, Turtle J, Bahr D, Jiang L, Wolcott M (2010) Thermal and mechanical properties of poly(3-hydroxybutyrate-co-3-hydroxyvalerate)/cellulose nanowhiskers composites. Polym (Guildf) 51:2652–2660
35. Manikandan NA, Pakshirajan K, Pugazhenthi G (2020) Preparation and characterization of environmentally safe and highly biodegradable microbial polyhydroxybutyrate (PHB) based graphene nanocomposites for potential food packaging applications. Int J Biol Macromol 154:866–877
36. Owen AJ, Heinzel J, Škrbić Ž, Divjaković V (1992) Crystallization and melting behaviour of PHB and PHB/HV copolymer. Polym (Guildf) 33:1563–1567
37. Öner M, Keskin G, Kızıl G, Pochat-Bohatier C, Bechelany M (2019) Development of poly(3-hydroxybutyrate-co-3-hydroxyvalerate)/boron nitride bionanocomposites with enhanced barrier properties. Polym Compos 40:78–90
38. Iulianelli GCV, David GS, Santos TNS, Sebastião PJO, Tavares MIB (2018) Influence of TiO2 nanoparticle on the thermal, morphological and molecular characteristics of PHB matrix. Polym Test 65:156–162
39. Yu HY, Qin ZY, Zhou Z (2011) Cellulose nanocrystals as green fillers to improve crystallization and hydrophilic property of poly(3-hydroxybutyrate-co-3-hydroxyvalerate). Prog Nat Sci Mater Int 21:478–484
40. Ten E, Jiang L, Wolcott MP (2012) Crystallization kinetics of poly(3-hydroxybutyrate-co-3-hydroxyvalerate)/ cellulose nanowhiskers composites. Carbohydr Polym 90:541–550
41. Dasan YK, Bhat AH, Ahmad F (2017) Polymer blend of PLA/PHBV based bionanocomposites reinforced with nanocrystalline cellulose for potential application as packaging material. Carbohydr Polym 157:1323–1332
42. Tang CY, Chen DZ, Yue TM, Chan KC, Tsui CP, Yu PHF (2008) Water absorption and solubility of PHBHV/HA nanocomposites. Compos Sci Technol 68:1927–1934
43. Montanheiro TLdoA, Montagna LS, Patrulea V, Jordan O, Borchard G, Ribas RG, Campos TMB, Thim GP, Lemes AP (2019) Enhanced water uptake of PHBV scaffolds with functionalized cellulose nanocrystals. Polym Test 79:106079

44. Valente BFA, Silvestre AJD, Neto CP, Vilela C, Freire CSR (2021) Effect of the micronization of pulp fibers on the properties of green composites. Molecules 26(18):5594
45. Malmir S, Montero B, Rico M, Barral L, Bouza R (2017) Morphology, thermal and barrier properties of biodegradable films of poly (3-hydroxybutyrate-co-3-hydroxyvalerate) containing cellulose nanocrystals. Compos Part A Appl Sci Manuf 93:41–48
46. Qasim U, Fatima R, Usman M (2020) Efficient barrier properties of mechanically enhanced agro-extracted cellulosic biocomposites. Mater Today Chem 18:100378
47. Lagaron JM, Catalá R, Gavara R (2004) Structural characteristics defining high barrier properties in polymeric materials. Mater Sci Technol 20:1–7
48. Calvino C, Macke N, Kato R, Rowan SJ (2020) Development, processing and applications of bio-sourced cellulose nanocrystal composites. Prog Polym Sci 103:101221
49. Dhar P, Bhardwaj U, Kumar A, Katiyar V (2015) Poly (3-hydroxybutyrate)/Cellulose Nanocrystal Films for Food Packaging Applications: barrier and migration studies. Polym Eng Sci 55:2388–2395
50. Zhang B, Huang C, Zhao H, Wang J, Yin C, Zhang L, Zhao Y (2019) Effects of cellulose nanocrystals and cellulose nanofibers on the structure and properties of polyhydroxybutyrate nanocomposites. Polym (Basel) 11:2063